diffraction and Aerometrics phase/Doppler. Appl. Opt. 26, 2144–2154
Dunn-Rankin, D.; Hoornstra, J.; Holve, D. J. 1986: In-situ non-Doppler laser anemometer particle sizer applied in heterogenous combustion. Paper 22.1. 3rd Int. Symp. Appl. laser anemometry Fluid Mech. Lisbon: LADOAN-Instituto Suberior Técnico
Holve, D. J. 1986: In situ measurements of flyash formation from pulverised coal. Combust. Sci. Tech. 44, 269–288
McDonell, V.; Milosavljevic, V.; Taylor, A. M. K. P.; Whitelaw, J. H. 1988: Mixing in small-scale non-premixed flames stabilised by swirl; the influence of fuel nozzle geometry. Report FS/88/23. Dept. Mech. Eng. Imperial College, London
McLaughlin, D. K.; Tiederman, W. G. 1973: Biasing correcting for individual realization of laser anemometer measurements in turbulent flows. Phys. Fluids 16, 2082–2088
Saffman, M. 1987: Automatic calibration of LDA measurement volume size. Appl. Opt. 26, 2592–2597
Shih, T. H.; Lumley, J. L. 1986: Second-order modelling of particle dispersion in a turbulent flow. J. Fluid Mech. 163, 349–363
Yeoman, M. L.; Azzopardi, B. J.; White, H. J.; Bates, C. J.; Roberts, P. J. 1982: Optical development and application of a two colour LDA system for the simultaneous measurement of particle size and particle velocity. In: Engineering Applications of Laser Velocimetry, Winter Annual Meeting. Phoenix (eds. Coleman, H. W.; Pfund, P. F.) pp. 127–136. New York: ASME

Received December, 18, 1988

Drag and lift coefficients evolution of a Savonius rotor

A. Chauvin and **D. Benghrib**

Université de Provence, Laboratoire des Systèmes Energétiques et Transferts Thermiques, Faculté Saint Jérôme, Avenue Escadrille Normandie Niemen 13397, F-Marseille Cedex 13, France

Abstract. The lift and drag coefficients of the rotating Savonius wind machine are determined from the pressure difference measured between the upper plane and the lower plane of a blade. Pressure measurements have been performed for two sets of experiments; the first one for $U_\infty = 10$ m/s and the second one for $U_\infty = 12.5$ m/s. In each case it is to be noted that a negative lift effect is present for low values of the tip speed ratio λ. The lift coefficient becomes positive when λ increases. The drag coefficient is of course always negative.

List of symbols

A	rectangular area of the wind tunnel
C_X	drag coefficient
C_Y	lift coefficient
$\bar{C}_X$	averaged drag coefficient
$\bar{C}_Y$	averaged lift coefficient
D	rotor diameter
h	rotor height
$R+r$	radius of rotation of a blade
Re	$(U_\infty \cdot D)/\nu$ Reynolds number
S	rotor projected area
U_∞	wind velocity
δ	central gap
λ	tip speed ratio
ν	cinematic viscosity
ϱ	density of air

1 Introduction

Many studies have been carried out concerning the Savonius rotor Newman (1974) and Ushiyama (1986), mainly experimental works in order to determine the torque and the power coefficients. The experimental knowledge of the instantaneous pressure field on the blades of the machine, during a complete rotation enables one to calculate these mechanical parameters. The pressure field measurements, associated to the vortex formation visualized close to the blades gives a good understanding of the evolution of these vortices Chauvin et al. (1987). The study presented here, based also on the measurements of the pressure field, leads to the determination of the lift and drag coefficients. Then we compare these results with those obtained with a rotating cylinder.

2 Drag and lift coefficients

2.1 Experiments

The tested machine is composed of two half cylindrical blades with a central gap (Fig. 1).

At each extremity, the rotor is limited by a circular disc of 150 mm diameter. The rotor is placed in an aerodynamic wind tunnel of rectangular cross section (0.8×0.8 m^2). The natural turbulency level is about: $5 \cdot 10^{-4}$. Pressure gauges

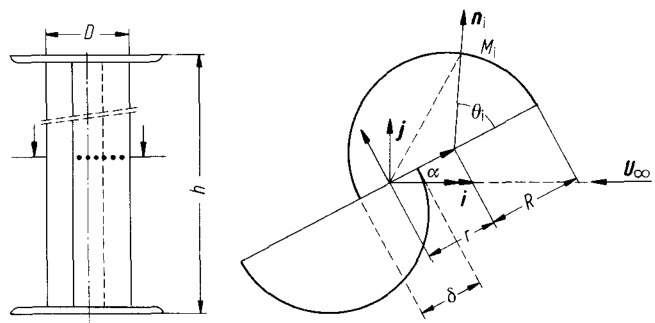

Fig. 1. The dimensions are: $D = 102$ mm, $h = 314$ mm, $\delta = 28$ mm

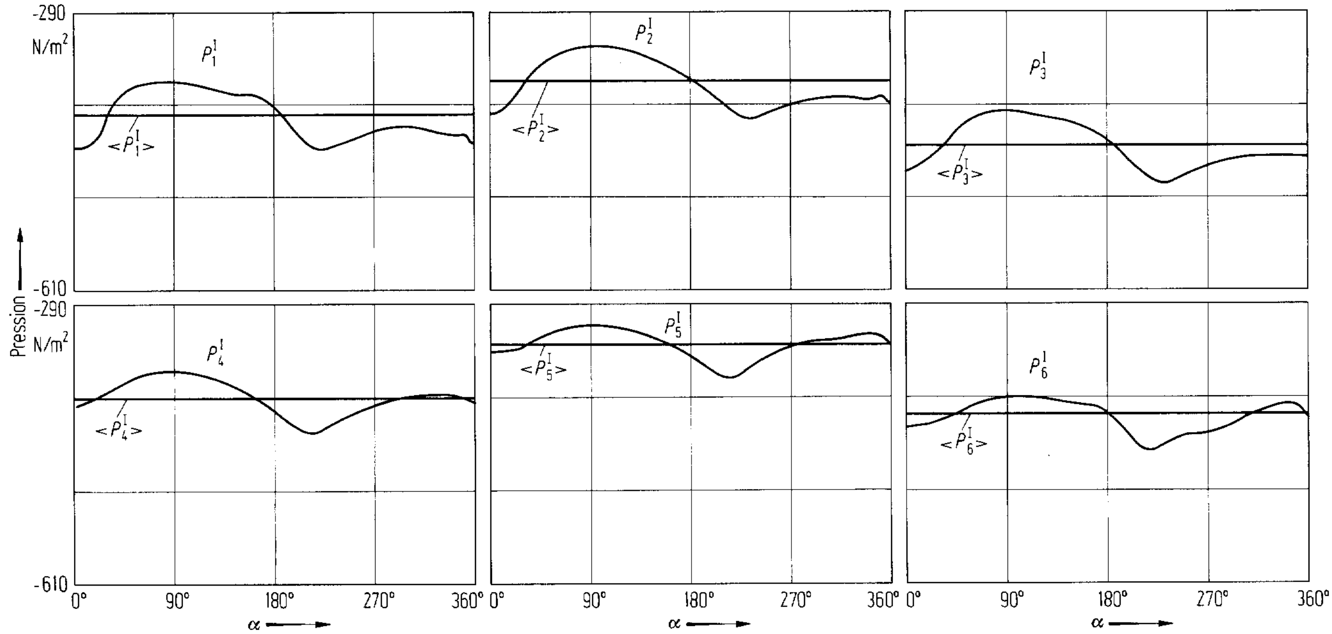

Fig. 2. Curves of pressure on the lower plane for 10 m/s

are located into six circular holes in the mid-plane of the blade cross-section. The pressure gauges are of piezoresistive type with thermal compensation. The signals are first amplified on the top of the blade and then transmitted to the outer measurement chain by means of rotating contacts. The rotating frequency is measured with a photo-diode installed at the axis end. Taking into account of the symetrical behaviour of the blades, during a complete rotation, the DP transducers are mounted only on one blade. Details of this experimental work are presented in a previous paper Chauvin et al. (1987). Figure 2 shows 6 DP traces. The zero pressure level is the atmospheric pressure one. Two sets of measurements have been performed: one for a flow speed $U_\infty = 10$ m/s and λ values respectively equal to 0.2, 0.4, 0.6, 0.71, and the other for $U_\infty = 12.5$ m/s and λ equal to 0.43, 0.7, 0.8, 1. The tip speed ratio λ is so defined:

$$\lambda = \omega (R + r)/U_\infty .$$

The frequency and the pressure signals registered simultaneously in a data acquisition system, can also be visualized on a memory oscilloscope. Then we obtain the instantaneous pressure field on each side of a blade for a complete revolution of the machine.

The blockage factor $\varepsilon = S/4 \cdot A$, defined by Alexander (1978) and Backwell et al. (1977) is here rough estimate 0.013. So the wind tunnel interference has been neglected, in a first approximation.

2.2 *Drag and lift coefficients*

Using the pressure measurements we have calculated the drag and lift coefficients of the rotor in the two experimental situations. The flow is assumed to be inviscid and two dimensional.

Drag and lift are obtained by integrating the various projections of aerodynamic forces along the two fixed directions $\boldsymbol{i}$ and $\boldsymbol{j}$. The drag and lift coefficients are respectively defined under the following form:

$$C_x = \frac{\Sigma_{i\varepsilon A+B} \boldsymbol{F}_i \cdot \boldsymbol{i}}{\frac{1}{2} \varrho S U_\infty^2} \tag{1}$$

$$C_y = \frac{\Sigma_{i\varepsilon A+B} \boldsymbol{F}_i \cdot \boldsymbol{j}}{\frac{1}{2} \varrho S U_\infty^2} . \tag{2}$$

During a half revolution, we distinguish the two blades by the letters (A) and (B). Then aerodynamic forces are noted:

$$\boldsymbol{F}_i^\beta = \Delta P_i^\beta \, \Delta S_i \, \boldsymbol{n}_i \tag{3}$$

where β equals (A) or (B) according to the blade under study ΔP_i^β is the pressure difference (Internal-External) at the M_i point. $\Delta S = R_i \Delta\theta_i$ is the surface element and $\boldsymbol{n}_i$ the external oriented unit vector normal to the blade.

From the expressions (1), (2) and (3) we obtain:

$$C_x = \frac{R\,h\,\{\Sigma(\Delta P_i^A - \Delta P_i^B)\cos(\theta_i + \alpha)\}\,\Delta\theta_i}{\frac{1}{2} \varrho S U_\infty^2} \tag{4}$$

$$C_y = \frac{R\,h\,\{\Sigma(\Delta P_i^A - \Delta P_i^B)\sin(\theta_i + \alpha)\}\,\Delta\theta_i}{\frac{1}{2} \varrho S U_\infty^2} . \tag{5}$$

The last expressions represent the instantaneous values of drag and lift coefficients, depending on the pitch angle α. According to the symmetrical behaviour of the blades it is sufficient to study the C_x and C_y evolution during one half of a complete revolution of the machine, α remaining in the range $(0, \pi)$. The more interesting and significant values of C_x and C_y are not the instantaneous, but the average values $\bar{C}_x$ and $\bar{C}_y$. They are obtained by averaging C_x and C_y during a half rotation.

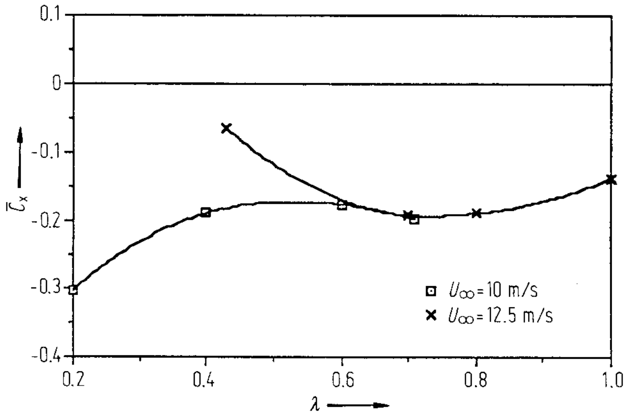

Fig. 3.

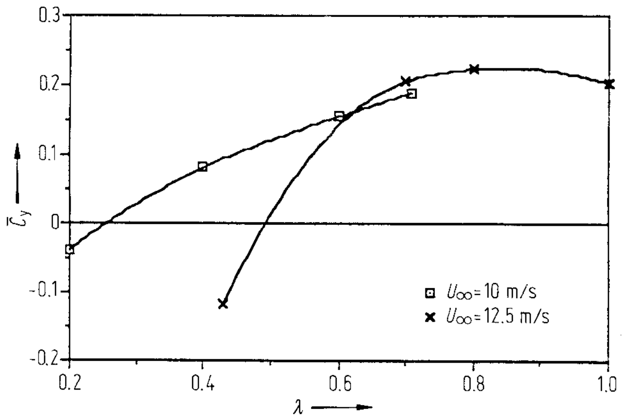

Fig. 4.

Figs. 3 and 4. The evolution of the drag and lift coefficients

3 Results

The expressions (4) and (5), based on the pressure measurements, are then computed in each experimental case. The curves presented in Figs. 3 and 4 show the evolution of the drag and lift coefficients.

First we notice that the drag coefficient $\bar{C}_x$ is always negative. This means that the drag resultant forces are of the same sense as the incident flow direction. This result agrees obviously with the physical situation.

At low values of the tip speed ratio, the lift coefficient $\bar{C}_y$ presents, for both Reynolds numbers, a negative contribution (more important when $Re = 8.7 \cdot 10^4$). Then $\bar{C}_y$ becomes positive for $\lambda \geq 0.25$ and $\lambda \geq 0.55$ when Re is $6.9 \cdot 10^4$ and $8.7 \cdot 10^4$ respectively. For large values of λ, $\bar{C}_y$ has approximately the same level in the two sets of experiments. At our knowledge, it is the first time that one can notice such a phenomenon. However a similar observation has been done in the case of a rotating cylinder Calamote (1984) and Charrier (1979). The last author, studying the Magnus effect, has found an inverse lift effect when the tip speed ratio is in the range between 0.1 and 0.5, associated to Reynolds numbers conditions lower than critical Reynolds numbers.

It would be very interesting to describe more precisely what happens for the low λ values, for instance $\lambda < 0.25$. It has not be done experimentally because of the technical difficulties to maintain constant the rotation frequency.

4 Conclusion

The calculation, in inviscid fluid flow, of the drag and lift coefficients, from the instantaneous pressure measurements on the blades, shows essentially an inverse lift effect associated to low values of the tip speed ratio λ. Such a result is to be compared to similar observations on a rotating cylinder. For a fixed Reynolds number, we notice that the Magnus effect appears when the values of the tip speed ratio are greater than a critical one λ_c. Of course, two sets of experiments, for the two wind velocities are not sufficient to describe the dependance of λ_c on the Reynolds number.

References

Alexander, A. 1978: Wind tunnel corrections for Savonius rotor. 2nd international symposium on wind energy systems. Paper E.6. pp. 69–80. Amsterdam

Backwell, B.; Sheldal, R. E.; Feltz, L. V. 1977: Wind tunnel performance data for two- and three-bucket Savonius rotors. In Sandia laboratories. Tech. Repport sand 76-0131 Albuquerque/New-Mexico-USA

Calamote, J. 1984: Effet de la rotation sur les cylindres tournants. Thèse de 3ème Cycle, I.M.S.T. Université d'Aix: Marseille

Charrier, B. 1979: Etude théorique et expérimentale de l'effet Magnus destinée à la propulsion Eolienne. Thèse de 3ème Cycle. Université de Paris VI

Chauvin, A.; Aouachria, Z.; Marchand, O. 1987: Champs des pressions sur les aubes d'une éolienne Savonius. Détermination des coefficients de moment et de puissance. Etude des émissions tourbillonnaires sur les aubes. J. Mec. Theor. Appl. 6, 827–842

Newman, B. 1974: Measurement on a Savonius rotor with variable gap. In: Wind energy devices. Canada: Proc. University of Sherbrooke, pp. 115–136.

Ushiyama, I.; Nagai, H.; Shinoda, J. 1986: Experimentally determining the optimum design configuration. Bull. J.S.M.E. 29, 258

Received January 17, 1989